Environmental Microbiology (2022) 24(4), 1818-1834

doi:10.1111/1462-2920.15977



# Parasitic infections by Group II Syndiniales target selected dinoflagellate host populations within diverse protist assemblages in a model coastal pond

Taylor R. Sehein , 1\* Rebecca J. Gast, 2 Maria Pachiadaki, 2 Laure Guillou 3 and Virginia P. Edgcomb 4

<sup>1</sup>MIT-WHOI Joint Program in Biological Oceanography, Cambridge and Woods Hole, MA.

<sup>2</sup>Department of Biology, Woods Hole Oceanographic Institution, Woods Hole, MA.

<sup>3</sup>Sorbonne Université & Centre National pour la Recherche Scientifique, Station Biologique de Roscoff, Roscoff, UMR7144, France.

<sup>4</sup>Department of Geology and Geophysics, Woods Hole Oceanographic Institution, Woods Hole, MA.

#### Summary

Protists are integral to marine food webs and biogeochemical cycles; however, there is a paucity of data describing specific ecological niches for some of the most abundant taxa in marker gene libraries. Syndiniales are one such group, often representing the majority of sequence reads recovered picoplankton samples across the global ocean. However, the prevalence and impacts of syndinian parasitism in marine environments remain unclear. We began to address these critical knowledge gaps by generating a high-resolution time series (March-October 2018) in a productive coastal pond. Seasonal shifts in protist populations, including parasitic Syndiniales, were documented during periods of higher primary productivity and increased temperature-driven stratification. Elevated concentrations of infected hosts and free-living parasite spores occurred at nearly monthly intervals in July, August, and September. We suggest intensifying stratification during this period correlated with the increased prevalence of dinoflagellates that were parasitized by Group Il Syndiniales. Infections in some protist populations were comparable to previously reported large singletaxon dinoflagellate blooms. Infection dynamics in

parasites through mixed protist assemblages and highlighted patterns of host/parasite interactions that better reflect many other marine environments where single taxon blooms are uncommon.

Salt Pond demonstrated the propagation of syndinian

#### Introduction

Coastal oceans are highly productive systems that support complex marine food webs and play important roles in the cycling of carbon and nutrients. Within these environments, protists are taxonomically diverse drivers of energy and nutrient flow through their activities as primary producers or as parasites, heterotrophs or mixotrophs that facilitate the trophic transfer of energy between prokaryotes (Bacteria, Archaea) and Metazoa (Aristegui et al., 2009) and can exert top-down controls on certain populations. Protists occupy varied ecological niches; however, the common trophic strategies of mixotrophy and symbioses (parasitism and symbiotic mutualistic associations), are often poorly understood and unrecognized in models of marine food webs (Jephcott et al., 2016; Scholz et al., 2016; Frenken et al., 2017; Stoecker et al., 2017). Elucidating the extent and consequences of specific protistan interactions is critical for understanding microbial community structure and dynamics, as well as overall ecosystem function in the global ocean.

Molecular marker surveys of the eukaryotic small subunit ribosomal RNA (SSU rRNA) gene over the past two decades indicate protist parasites are abundant and likely to play significant roles in diverse marine ecosystems. For example, the Tara Oceans project surveyed the tropical sunlit and mesopelagic ocean and showed that parasitic protist groups accounted for up to 59% of total heterotrophic protist SSU rRNA gene richness and approximately 53% of abundance. Among these parasitic sequences, 89% of picoplankton diversity and abundance were affiliated with Syndiniales Groups I and II (phylum Dinoflagellata) (Pawlowski et al., 2012; de Vargas et al., 2015). The Malaspina-2010 Expedition found that four protist groups accounted for 69.6% of

Received 13 July, 2021; accepted 13 March, 2022. \*For correspondence. E-mail tsehein@whoi.edu; Tel. (508) 289 3064.

sequencing tags in the bathypelagic global ocean, and Group II Syndiniales sequences were the most highly represented, and phylogenetically diverse group in most Malaspina samples (Pernice et al., 2015). Similar results were obtained in other environmental surveys of polar regions and oxygen-minimum zones (Orsi et al., 2012; Duret et al., 2015; Cleary and Durbin, 2016; Suter et al., 2022). Collectively, surveys of SSU rRNA gene signatures suggest Syndiniales are abundant and ubiquitous in both coastal and open ocean environments and likely play a major role in those marine food webs (e.g. Lopez-Garcia et al., 2001; Massana et al., 2004; Not et al., 2007; Edgcomb et al., 2011; de Vargas et al., 2015; Pernice et al., 2015). Very little is known about the enigmatic Syndiniales lineages, beside the fact that all species formally described to date have a parasitic lifestyle (Cachon 1964; Guillou et al., 2008). A few of them are known to be an important cause of mortality for microbial eukaryotes and Metazoa (Skovgaard et al., 2005; Stentiford and Shields, 2005; Chambouvet et al., 2008).

Fundamental challenges when studying syndinian parasites and putative host interactions are their unresolved taxonomy and the paucity of morphological markers for different clades within this order. Syndiniales includes five distinct taxonomic groups (Guillou et al., 2008). Sequences from environmental datasets are most commonly assigned to Syndiniales Groups I and II, which include eight and >100 clades, respectively (Guillou et al., 2008; Cai et al., 2020). Group I, which includes the syndinian genus Eudoboscquella, is associated with infections of ciliates (Bachvaroff et al., 2012). The Amoebophrya species complex is the only described Group II Syndiniales genus, and this taxon is known to infect other dinoflagellates (Chambouvet et al., 2008; Guillou et al., 2008; Cai et al., 2020). Recent expansion of environmental sequence data in public databases suggests that the Amoebophrya species complex is affiliated with multiple clades within Group II, indicating that the group's taxonomy should be revisited, as well as the definition of the genus (Guillou et al., 2008; Cai et al., 2020). Other known hosts of syndinian parasites include radiolarians and copepods (Skovgaard, 2014; Brate et al., 2012); however, there are many clades within both Groups I and II that remain known only by their marker gene sequences and no information is available on host taxa.

Group II Syndiniales infection cycles have been described for a limited number of cultured isolates and environmental populations infecting dinoflagellates, with all belonging to the Amoebophrya species complex (Cachon, 1964; Cachon and Cachon, 1970; Miller et al., 2012). Infections lead to host mortality within several days, releasing nutrients to the environment both as

particulate and dissolved organic matter; however, the presence of syndinian parasites within the dormant resting stage of the dinoflagellate host, Scrippsiella acuminata, have been observed in culture (Chambouvet et al., 2011a,b). Infections generate dozens to hundreds of new propagules (dinospores) that are between 1 and 12 µm in diameter. Culture-based studies suggest dinospores survive only a few days after their release (Coats and Park, 2002). Assuming the life cycles of other uncultured Group II Syndiniales are similarly short, the dominance of their sequences in molecular datasets suggests their production in marine ecosystems is fairly constant.

An outstanding ecological question regards the impact of syndinian infections on protist populations and on the overall protist community. Previous studies of syndinian ecology have focused on a limited number of hosts through microscopic observations; however, the small size and lack of defining morphological features make dinospores and early stage infections difficult to identify and enumerate. Catalysed reporter deposition fluorescence in situ hybridization (CARD-FISH) is a more sensitive approach than light microscopy and has been used to successfully quantify free-living dinospores and infections in coastal, open ocean, and oligotrophic ocean water masses (Chambouvet et al., 2011b; Siano et al., 2011; Velo-Suarez et al., 2013). To date, several CARD-FISH probes have been designed to detect syndinian parasites, and one probe targets 73 of the 125 clades of Group II Syndiniales (ALV01; Chambouvet et al., 2008). Applications of CARD-FISH show that Group II parasite infections increase in abundance during the peak through the termination of some dinoflagellate blooms, including some harmful algal bloom taxa (Coats and Bockstahler, 1994; Coats and Park, 2002; Velo-Suarez et al., 2013). This suggests that syndinian parasites may exert top-down pressure on bloom-forming taxa. In the Penzé Estuary (Roscoff, France), up to 46% of dinoflagellates were infected (average of 21%) over a 3-month period during the summer (Chambouvet et al., 2008). Infection ratios were similar among the five dinoflagellate species that could be distinguished based on morphology, including the toxic alga Alexandrium minutum. Based on observed characteristic predatorprey dynamics in coastal settings, proliferation of parasite infections should occur when there is a high concentration of preferred hosts (Velo-Suarez et al., 2013).

CARD-FISH probes and epifluorescent microscopy can highlight interactions between hosts with distinct morphologies (Siano et al., 2011) and Group II Syndiniales parasites for which clade-specific probes have been designed (Chambouvet et al., 2008). Co-occurrence network analyses can be used to infer putative host-parasite interactions based on the co-presence of host and

parasite taxa. Recent research has hypothesized that syndinian parasites may infect diatoms (Sassenhagen et al., 2020) as well as the marine haptophyte, Phaeocystis (Christaki et al., 2017; Torres-Beltran et al., 2018). These findings indicate the host range for Group II Syndiniales could be broader than previously thought and encourages exploration of a broader range of marine systems.

Salt Pond (Falmouth, MA, USA) was selected for a highresolution time series study of syndinian infection dynamics because it is a good model for a typical, productive coastal site in the temperate Atlantic. Unlike previous studies of Group II Syndiniales that targeted regions where blooms of dinoflagellate hosts were prominent, little was known about the protist communities in Salt Pond and the impacts of Group II Syndiniales on individual protist populations. We combined molecular marker gene analyses, fluorescence in situ hybridization microscopy, and data on water chemistry to water samples collected every 3 days from March to October 2018. This timeframe was selected to capture periods of increased putative host cell densities, including anticipated spring and fall blooms of primary producers that are typical of the region, as well as mid-summer, temperature-driven stratification that concentrates protist cells across the oxic/anoxic interface (Bazylinski et al., 2000). We hypothesized that in Salt Pond, Group II Syndiniales infections would propagate more efficiently when there were higher concentrations of host populations.

# Results

Seasonality and environmental conditions in Salt Pond

Temperature and salinity increased from spring into summer at the shallowest depth we sampled in Salt Pond (2 m below the surface), with salinity values at 3 m and 4 m more uniform across the time series (Fig. 1; Table S1). Oxygen concentrations declined with depth beginning in May, with undetectable values shoaling to approximately 2 m on 16 August and these conditions persisted until 4 September. Ammonium was depleted from all three depths beginning on 14 May, with concentrations remaining low until 30 July. Ammonium then began to accumulate in low-oxygen and anoxic samples collected at 4 m. Concentrations of nitrate and nitrite were highest in spring months and were depleted at all sample depths in the summer and fall (Fig. 1; Table S1).

Spatial and temporal assessments of protist community composition

Barcoded iTag libraries targeted the hypervariable V4 region of the 18S SSU rRNA gene. Across the time series, libraries for 339 samples were sequenced,

generating 9 317 051 reads that were catalogued into 9196 amplicon sequence variants (ASVs; Table S2). ASVs were manually curated to remove sequences annotated only to Eukaryota without higher taxonomic resolution, Metazoa, and red and green macroalgae, leaving 6570 ASVs for protistan community analyses. Trends in community composition revealed seasonal shifts in the relative abundances of major groups including Cercozoa, chlorophytes, ciliates, dinoflagellates, and stramenopiles (Fig. 2B). The relative abundances of these groups were similar across the three depths at each sampling event, with several exceptions. Chlorophytes were more abundant at the 2 m depth in early spring, ciliates were most abundant at 4 m across most of the time series, and cryptophytes were most abundant at 4 m in late July and early August.

The relative abundances of Group II Syndiniales parasite sequences (Fig. 2A) exhibited periodicity across the times series. Local peaks in Group II Syndiniales sequences coincided with occurrence of dinoflagellate-dominated protist communities and with elevated infection events recorded using CARD-FISH and epifluorescence microscopy in July, August, and September. Group I Syndiniales sequences, commonly associated with ciliate infections, were most abundant in sample data sets at 3 and 4 m in September and October. Sequences annotated to Group III Syndiniales, whose parasitic function and hosts are unknown, were nearly undetectable at 2 m throughout the time series, but their sequences were abundant at 3 and 4 m from mid-May to mid-June.

Non-metric multidimensional scaling analysis of the iTag libraries indicated protist communities grouped by sampling month (Fig. 3). Abiotic factors related to seasonal changes, including temperature, salinity, dissolved oxygen, wind direction, maximum wind gust, and combined nitrate and nitrite concentrations, were all significantly associated with sample clustering. We calculated positive correlations between dissolved oxygen and nitrate + nitrite, day length, and wind direction, which likely covary due to seasonal patterns at temperate latitudes. Strong negative correlations were identified between temperature and dissolved oxygen and nitrate + nitrite, corresponding to changes in the water column associated with thermohaline stratification (Fig. S2). Depth did not significantly influence the grouping of samples across the ordination plot.

Parasite enumeration: free-living spores and infected host morphologies

The seasonal impacts of Syndiniales parasites on protist populations were evaluated by using CARD-FISH and fluorescence microscopy to enumerate both infected

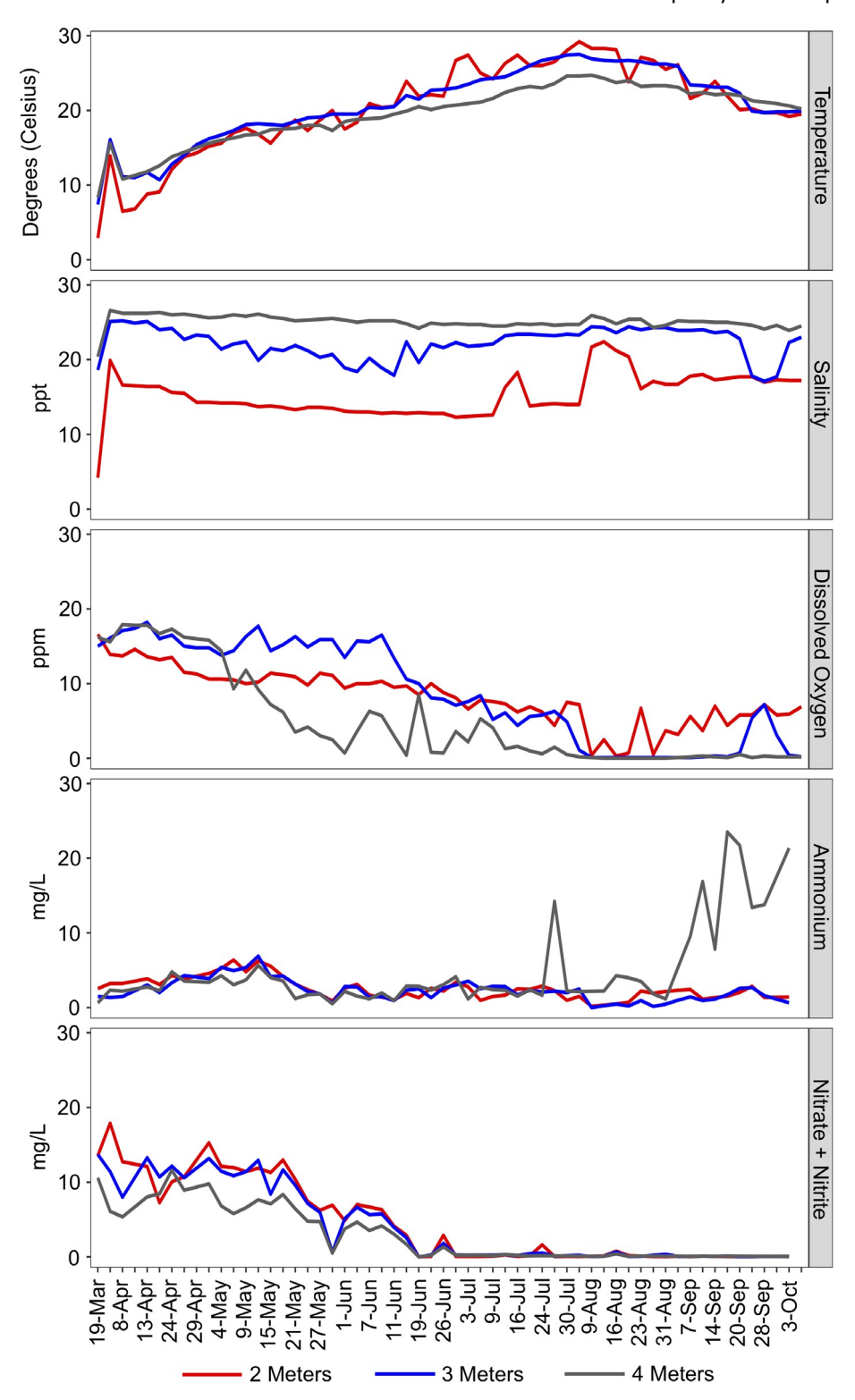


Fig. 1. Abiotic variables measured across the time series from the three sampling depths. Temperature, salinity, and dissolved oxygen were measured by hand-held YSI (YSI Pro2030, Ohio, USA). Water chemistry samples for ammonium and nitrate and nitrite were filtered and analysed on an O.I. Analytical Flow Solutions IV auto analyser.

hosts and free-living dinospores. For infected host counts, 283 filters spanning the March-October 2018 sampling dates were hybridized from the three depths sampled (Fig. 4). Filters from 27 April to 11 May were not

inspected because no Syndiniales amplicons were present in the corresponding iTag samples. In silico analysis of the ALV01 probe sequence revealed the probe matched 341 of 438 Group II ASVs from Salt Pond,

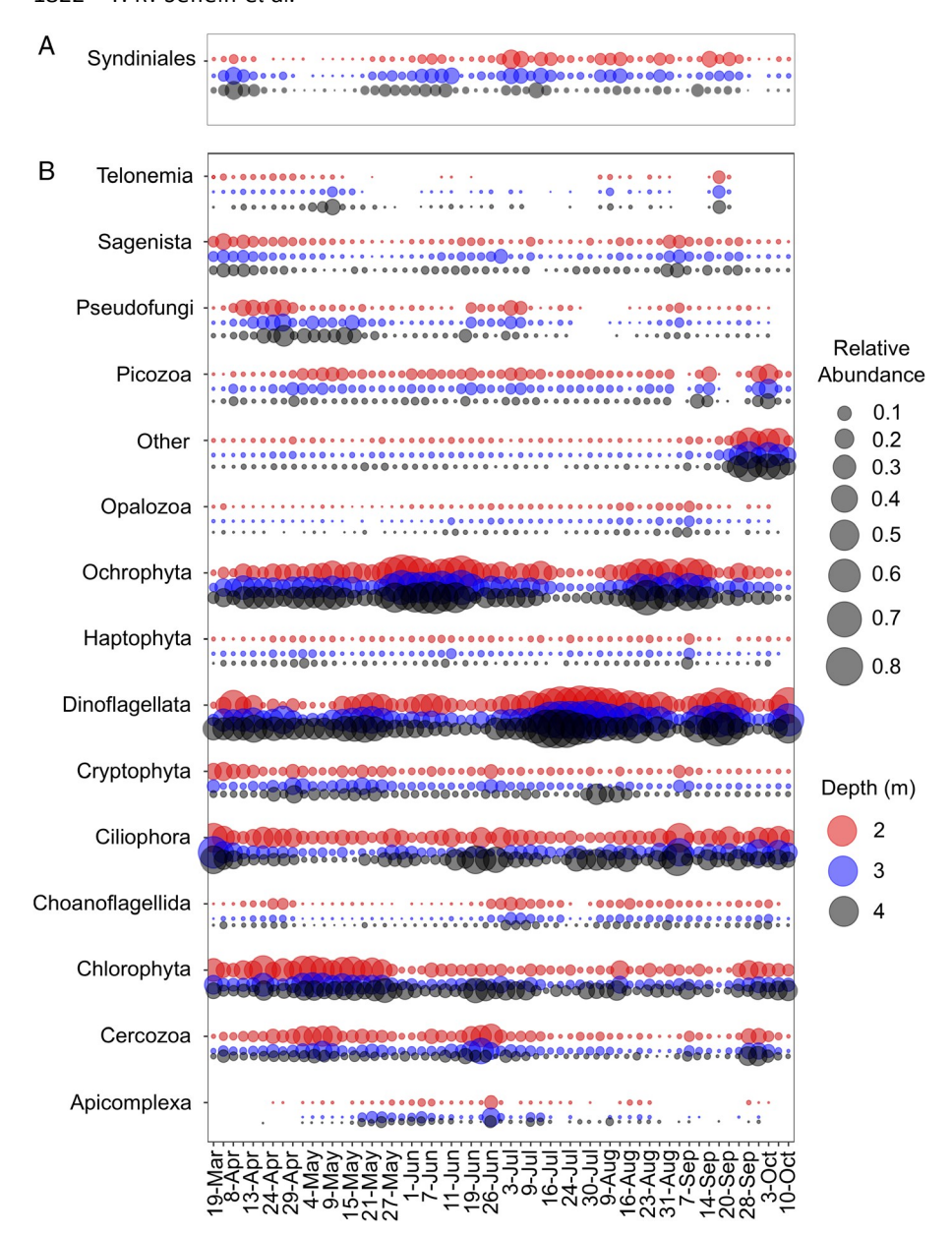


Fig. 2. Relative abundances of reads annotated to (A) Syndiniales and (B) phyla in 18S rRNA marker gene libraries collected across the times series. Reads annotated unassigned alveolates, Perkinsea, Amoebozoa, Apusozoa, unassigned Archaeplastida, Streptophyta, Discoba. Centroheliozoa, Katablepharidophyta, unassigned opisthokonts, fungi, Mesomycetozoa, and unassigned stramenopiles are included in 'Other.'

representing 93.4% of Group II Syndiniales reads. Infections were detected in a small fraction of the overall protist community throughout most of the time series, with three infection events occurring significantly above background levels at nearly monthly intervals in July, August, and September. The highest prevalence of infected protists, 2.56%, was observed on 13 August at 3 m depth. Additional peaks in infections occurred on 3 July and 14 September at the 2 and 3-m depths, illustrating periodicity in infection cycles across the summer months of 2018. Host morphologies were diverse and represented a range of athecate and thecate dinoflagellates, including heterocapsids, scrippsielloids, and dominant large athecate cells based on microscopic observations of

characteristic morphologies (Fig. S3). Infection frequencies were calculated for the three morphotypes (Fig. S4). No infections of other dominant protist groups were evident, including ciliates and diatoms.

Because most infections occurred at the 2 m depth, a subset of filters around the three elevated infection periods was also selected to quantify free-living spore concentrations. Dinospore concentrations were enumerated in 34 samples and were found to reach similar local maxima concurrent with host infections on 3 July (335 000 spores L<sup>1</sup>) and 14 September (139 200 spores L<sup>1</sup>). No increase in spore concentration was observed for sampling dates on or around the 13 August infection peak (Fig. 4).

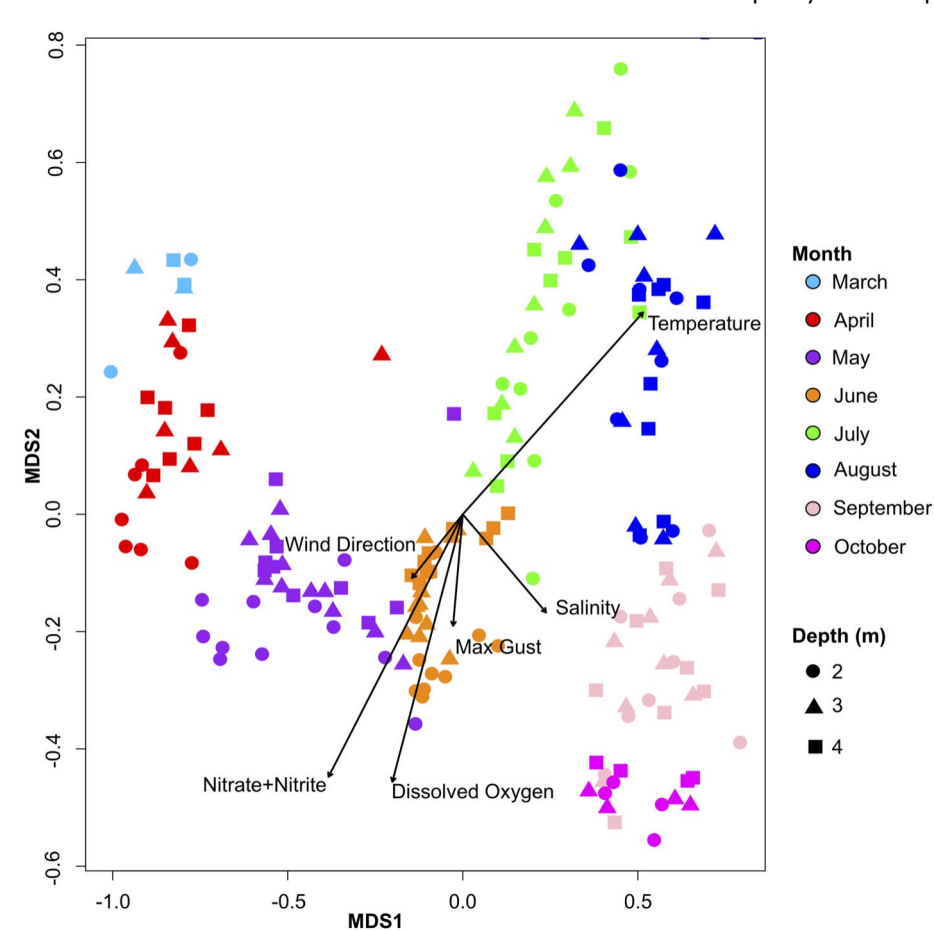


Fig. 3. A nonmetric multidimensional scaling (NMDS) plot of 18S rRNA marker gene libraries collected across the time series and three depths. The distance matrix was constructed using Bray-Curtis dissimilarity. Vectors indicating significant correlations with environmental variables are displayed (P < 0.05).

# Clustering analyses and protist community succession

Additional statistical analyses examined the relative abundance of protist taxa in the iTag libraries for samples collected from 2 m depth where most infections were observed (Fig. 4). 'Universal' primers have the potential to miss some fraction of the in situ community, and in this case, it appeared to miss a dominant euglenoid morphotype that microscopy revealed formed blooms of millions of cells L<sup>1</sup> at multiple time points across the time series at the 3- and 4-m depths. These euglenoids were not infected by Group II Syndiniales. Given the general similarities of protist communities across depths illustrated by the NMDS analysis, we focused attention on iTag libraries from the 2 m samples where observed infections were highest, to characterize cohorts of cooccurring protist populations.

The k-medoids method was used to parse the iTag libraries into patterns of co-occurring protist taxa. This analysis revealed four cohorts representing distinct protist communities that appeared at different times across the sampling period (Fig. 5). The taxonomic diversity of each cluster is listed in Table S3. Clusters were identified across the time series by calculating z-scores, which

describe the combined presence (positive values) and absence (negative values) of all taxa within each cluster. Here, only the positive values are presented, indicating the taxa within a cluster were present above mean baseline values on a given sampling date. Cluster 4 was present in both early spring and early fall samples, which suggests these protist taxa exhibit temporal periodicity in the pond, perhaps influenced by temperature. Other clusters, including clusters 1, 2, and 3, occurred once during the time series, and persisted for approximately 1 month each.

# Syndiniales diversity during infection events

A total of 470 ASVs were annotated to the order Syndiniales, representing 7.15% of all protist taxonomic annotations across the time series. The abundance of Syndiniales reads within individual iTag barcode libraries ranged from zero on multiple dates to 19.39% on 8 April (Fig. 2A). Like the overall protist community, the relative abundance of sequences from Syndiniales strains varied across the time series. In particular, Group II Syndiniales clade diversity differed during the three infection events

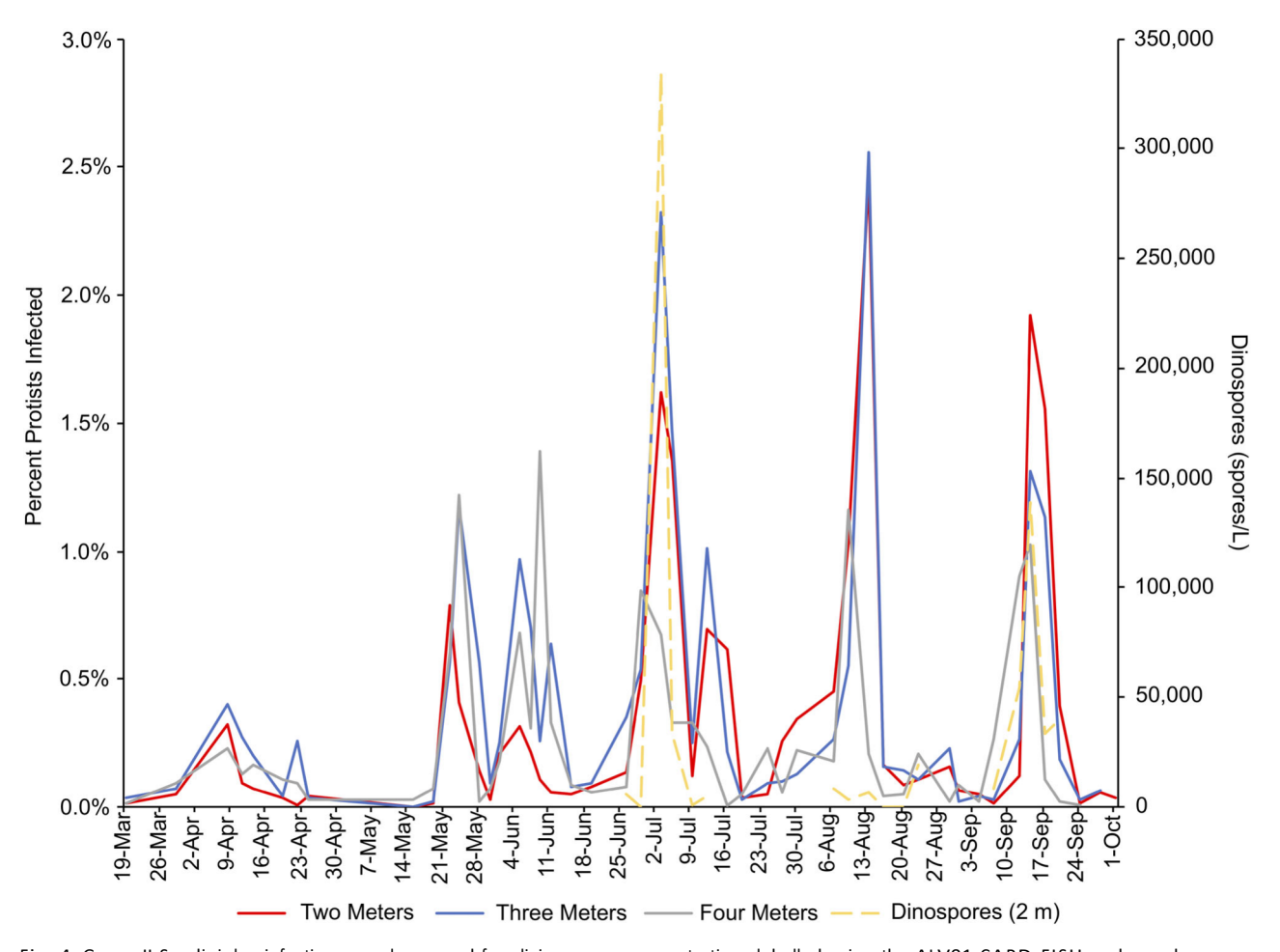


Fig. 4. Group II Syndiniales infection prevalence and free-living spore concentrations labelled using the ALV01 CARD-FISH probe and enumerated by epifluorescent microscopy. Fractions of protists infected from the three sampling depths across the time series are presented (solid lines, primary axis) in addition to the concentration of parasite spores collected at 2 m during the infection peaks in July, August, and September (dashed line, secondary axis).

observed in July, August, and September (Fig. S5). Reads annotated to Group II clade 2 represented approximately 97% of all Group II Syndiniales on 3 July. Likewise, over 94% of Group II Syndiniales were annotated to clade 30 on 14 September. These mono-clade infection events provide key information about specific host-parasite interactions when putative hosts can be identified morphologically or by using additional FISH analyses. On the other hand, the 13 August infection peak was uniquely diverse, with reads represented by six Group II Syndiniales clades (1, 2, 4, 5, 14, 22) and unidentified Group II sequences.

# Discussion

The coastal tidal pond, Salt Pond (Falmouth, MA, USA; Fig. S1) is an example of a highly productive coastal ecosystem, with features resembling many other coastal

ponds formed by glacial activity in the region. Salt Pond was used as a natural laboratory to study parasitism by Syndiniales during the seasonal succession of protist populations, as well as the effects of stratification on parasitic protist interactions. Salt Pond has been surveyed extensively by researchers interested in magnetotactic bacteria (Simmons et al., 2004; Simmons et al., 2007; Moskowitz et al., 2008) and sulfur compounds that accumulate in the chemocline (Wakeham et al., 1984; Zimmelink et al., 2006); however, little was known about its protist community, including the diversity of Group II Syndiniales, or how stratification might influence protist distribution and syndinian interactions with hosts in the water column. Based on the previous studies of syndinian impacts on bloom-forming dinoflagellate populations (Chambouvet et al., 2008; Siano et al., 2011; Velo-Suarez et al., 2013), we hypothesized that infections would be more prevalent during seasonal bloom cycles and periods of stratification when most hosts were

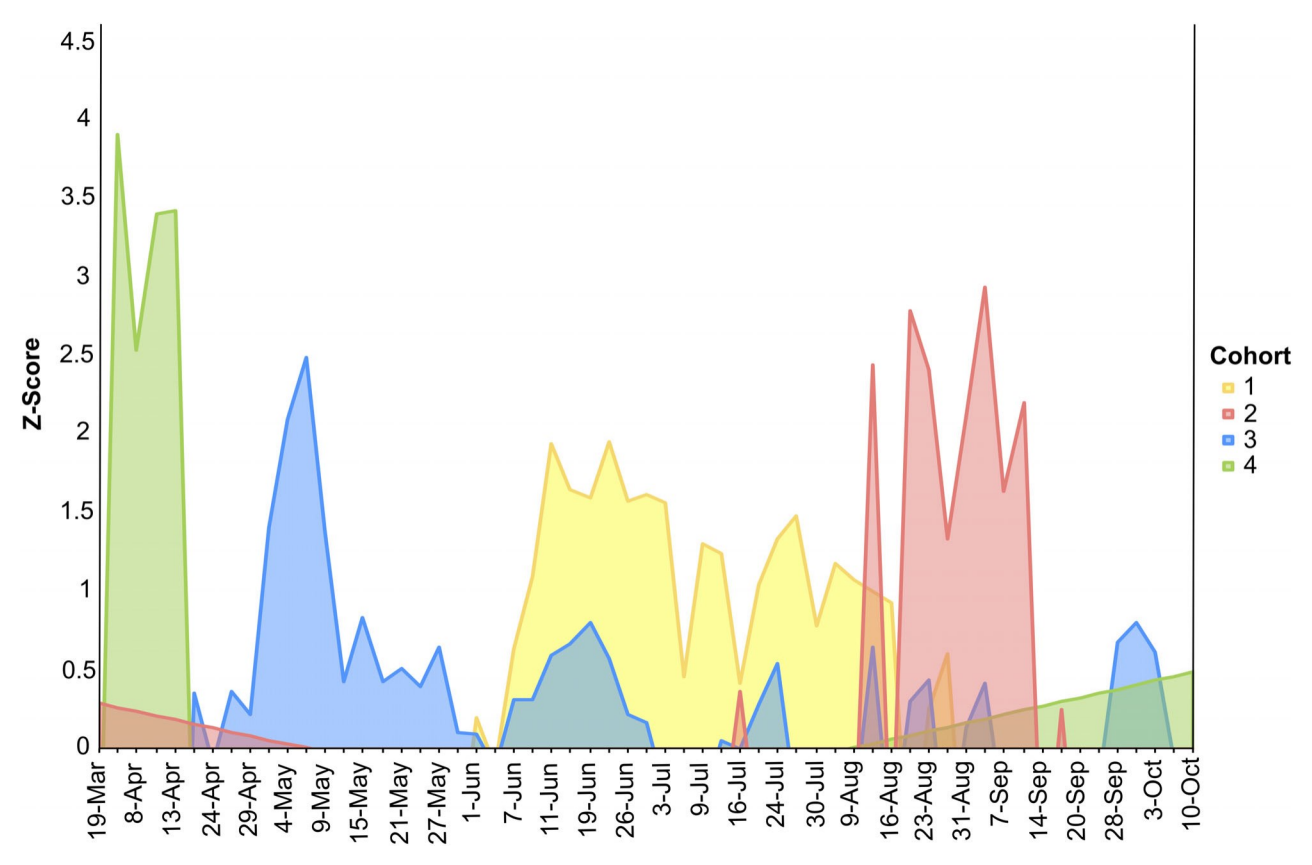


Fig. 5. The summed z-scores show the succession of eukaryotic cohorts across the time series based on the read abundances of taxa within each cohort. The z-score for each taxon was calculated as the difference between the observed and mean number of reads divided by the stan-dard deviation and described the frequency of reads that differed from the averaged baseline. Positive z-scores described when taxa from the cohorts were present at 2 m.

concentrated in the upper water column. Our time series sampling captured periods of increased primary production (spring and fall blooms) as well as stratification in the late summer.

Intensifying stratification alters environmental variables in Salt Pond

Salt Pond is approximately 5.5 m deep at its deepest point and the water column is structured by thermohaline stratification between mid-July and mid-September. Tidal mixing of freshwater from groundwater inputs and saltwater from the neighbouring Vineyard Sound results in waters that are more saline with depth, and often cooler (Fig. 1). Differences in the temperatures recorded at 2and 4-m increased from mid-June to mid-September, with intensifying stratification of the water column.

Oxygen concentrations in the pond varied across the time series. Oxygen increased with depth in the early spring (19 March to 7 May) suggesting elevated primary production and vertical mixing with oxygenated surface waters, but concentrations declined rapidly at 4 m

through May. Concentrations at 3 m declined in mid-June, concurrent with increased stratification of the water column. Concentrations of ammonium and both nitrate and nitrite were measured at the three sampling depths across the time series and exhibited declines beginning in mid-May. Ammonium concentrations later increased at 4 m depth between September and the end of the time series. These trends in oxygen and nitrogen concentrations during the intensification of thermohaline stratification in the summer months are consistent with publications on Salt Pond from decades ago (Wakeham et al., 1984, 1987), suggesting that Salt Pond is a relatively stable system with changes in environmental parameters primarily driven by seasonal forcing.

Seasonal influences on the Salt Pond protist community

Salt Pond protist communities included diverse assemblages of dinoflagellates, diatoms, ciliates, chlorophytes, cryptophytes, and cercozoa (Fig. 2B). While the relative abundance of taxonomic groups in iTag libraries can be biased by primer choice (Balzano et al., 2015), the number of gene copies per cell (Prokopowich et al., 2003; Gong and Marchetti, 2019), and amplification methods, examination of relative abundances of different protist taxa provides a view into general protist community trends. In Salt Pond, ASVs affiliated with dinoflagellates and diatoms comprised the two most abundant protist groups and exhibited niche differentiation across the time series. Shifts from diatom-dominated to dinoflagellate-dominated communities have been observed in many other marine settings (Trigueros and Orive, 2001; Zhou et al., 2017; Spilling et al., 2018). However, the timing of these shifts in association with biotic interactions (such as parasitism) is less understood.

In temperate coastal settings, a period of elevated primary production termed the spring bloom occurs in response to warming waters, decreased vertical mixing, and replete nutrients (Sverdrup, 1953; Mallin et al., 1991; Yoshie et al., 2003; Silva et al., 2009; Jin et al., 2013; Carstensen et al., 2015). Spring protist communities described by the iTag libraries in Salt Pond were dominated by diatoms and chlorophytes (Fig. 2), suggesting a bloom of these primary producers. The elevated oxygen concentrations throughout the water column recorded between 19 March and 7 May also indicate increased primary production. A second shift toward a diatomdominated community occurred in the transition from late August to early September when peak stratification occurred (9 August to 24 September) and sub-oxic conditions shoaled to approximately 2 m. During this peak stratification ammonium, nitrate and nitrite were depleted in the upper water column (0.0-2.89 mg l1, average 1.23 mg  $l^{1}$ ; 0.01–0.85 mg  $l^{1}$ , average 0.14 mg  $l^{1}$  for ammonium and nitrate + nitrite, respectively). Diatoms abundant in August and September (Chaetoceros, Navicula, and Skeletonema) differed from species present during the spring bloom (Thalassiosira, Pinnularia, and Leptocylindrus) and may have adaptations to nutrientlimited conditions or the ability to scavenge nutrient hotspots created by biotic interactions (i.e. parasitism) between other protists.

Many dinoflagellates are adapted to nutrient-limited environments due to their metabolic flexibility (mixotrophy in many species). iTag libraries from late June until mid-August and between September and the end of October indicated protist communities were dominated by dinoflagellates at all depths sampled. Dinoflagellates are known to have high numbers of SSU rRNA gene copies (Not et al., 2009; Galluzzi et al., 2010; Lin, 2011; Pernice et al., 2013) and this may lead to overestimation of their relative abundance; therefore, we enumerated the dominant morphotypes (heterocapsid, scrippsielloid, and large athecate cells; Fig. S3). Dinoflagellate populations included known Group II Syndiniales hosts such as Alexandrium sp. (Nishitani et al., 1985; Jacobson, 1987;

Sengco et al., 2003), Gonyaulax sp. (Kim et al., 2008; Siano et al., 2011), Gyrodinium sp. (Jacobson, 1987; Coats et al., 1996), Heterocapsa sp. (Kim, 2006; Chambouvet et al., 2008), Scrippsiella sp. (Coats et al., 1996; Chambouvet et al., 2011a,b; Li et al., 2014), and Prorocentrum sp. (Maranda, 2001; Salomon et al., 2009). These findings suggest that increased stratification observed in the summer months promoted proliferation of primarily dinoflagellate protist populations that are susceptible to Group II Syndiniales infections.

Reads affiliated to Group II Syndiniales ASVs (Fig. 2A) and parasitic infections (Fig. 4) were most abundant when other dinoflagellate groups dominated. There are many factors that can contribute to Syndiniales cell concentrations and their representation in marker gene libraries across the time series, including infections of host populations, changes in gene content during different life stages of both the host and the parasite, and the shortlived survival of free-living spores. Syndinian diversity in Salt Pond also included sequences annotated to Groups I and III. Reads annotated to these groups were more abundant in early spring and from late May to mid-June, when communities were not dominated by dinoflagellates. Ciliates, thought to be the preferred host phylum for Group I Syndiniales (Guillou et al., 2008; Bachvaroff et al., 2012), were present in iTag libraries across the time series; however, there was no clear pattern of co-occurrence between individual ciliate and Group I Syndiniales ASVs. Reads annotated to Group III Syndiniales were more abundant in the late spring and, unlike reads annotated to Group II, were more highly represented in libraries collected at 4 m depth than at 2 m depth. There are no known hosts for Group III Syndiniales; therefore, observations of this taxon require additional investigation to better understand the ecological relevance in Salt Pond.

A seasonal impact on community composition was evident. Non-metric multidimensional scaling (NMDS: Fig. 3) analysis of iTAG libraries showed that samples grouped closely by month, with no distinction between sampling depths. Environmental vectors fitted to the NMDS ordination indicated that temperature, salinity, dissolved oxygen, wind direction, maximum wind gust, and combined nitrate and nitrite concentrations were all significant factors structuring community composition. Among these, the most significant variables either directly enhanced seasonal stratification (e.g. temperature, salinity) or were the result of it (e.g. dissolved oxygen, nutrient concentra-Previous research suggested stratification tions). (Margalef et al., 1979) and diverse metabolic capabilities of dinoflagellates (Smayda and Reynolds, 2003; Kremp et al., 2008) promote dinoflagellate-dominated communities in coastal systems. In Salt Pond, intensifying stratification led to a shift in the protist community toward dinoflagellates in July, August, and September.

Spatial and temporal variation in Group II Syndiniales abundances

Although ALV01 did not target all Salt Pond Group II ASVs (it covered 341/440), it was still useful for observing high-resolution changes in abundance of members of this protist group in a coastal setting. Infections were sparse in the early spring, but as biomass increased and stratification intensified in the summer months, abundances and infections increased (Fig. 4). Periodic infections coincided with alternating blooms and crashes of putative host taxa ASVs observed at near-monthly intervals. Infections often concentrated nearer to the surface and were more abundant at the 2- and 3-m depths than at the 4 m depth in July, August, and September, suggesting Group II Syndiniales in Salt Pond preferentially target thecate and athecate dinoflagellate hosts that were found in more oxic waters. Microscopy revealed common host morphotypes that were consistent with heterocapsids, scrippsielloids, and large athecate cells (Fig. S3). These same infected morphotypes were also observed in samples from 4-m depth, but were less abundant there, and may have been sinking cells from the surface. Consistent with previous studies, no ciliate morphotypes appeared to be infected by Group II syndinian parasites targeted by the ALV01 probe.

A lower proportion of infections observed at the 4 m depth in the summer months (June to September) could be partially explained by abundant unidentified and possibly mixotrophic, green euglenoids (10<sup>6</sup> cells L<sup>1</sup>) pre-sent in the lower oxygen samples (at 3 and 4 m depth), which were not infected by the Group II Syndiniales para-sites. These euglenoids were not detected by our eukary-otic primers in the iTag libraries; therefore, a future study is needed to evaluate the role of these euglenoids in micro-oxic to anoxic marine systems like Salt Pond.

Infections lead to the release of dozens to hundreds of infective parasite spores per lysed host, which could be an important source of particulate organic matter for the local microbial community (Edgcomb, 2016). Group II Syndiniales dinospore concentrations were enumerated in samples collected from the 2 m depth around the July, August and September infection events, using the ALV01 CARD-FISH probe. Counts of dinospores were highest on the sample dates concurrent with the July and September infection peaks (Fig. 4). These observations differ from previous studies that showed peaks in dinospore concentrations that lagged peaks in infections by several days. The lag is caused because spores are released from infections approximately 24 to 48 h after initiation of an infection (Chambouvet et al., 2008; Velo-Suarez et al., 2013). Given the 2- to 3-day interval between our sampling dates, it is possible that spore concentrations were higher than we observed in the day(s)

following the infection events, on days that we did not sample. It is also possible that released spores were rapidly removed from the system by mortality, grazing, or hydrodynamic processes. No peak in dinospores was observed during the August infection event (Fig. 4), which may indicate removal processes that exceeded production during this time period.

Cohorts highlight potential environmental and biological drivers of succession

Four cohorts of co-occurring protist taxa, consisting of 284 ASV taxonomic bins annotated to the highest level possible (Table S3), were classified using the k-medoids clustering method. The timing and composition of these cohorts were compared with the environmental measurements and biological observations to generate new hypotheses about the factors influencing protist community structure and succession in Salt Pond.

The timing of the July and August infection events coincided with the presence of cohort 1, which extended from early June to mid-August. Cohort 1 consisted of 31 species of dinoflagellates, including the genera Alexandrium sp., Gyrodinium sp., Heterocapsa sp., and Scrippsiella sp. These taxa are known to host Group II Syndiniales parasites and have been associated with reports of infections in diverse coastal systems including the Chesapeake Bay (Maryland, USA; Coats and Bockstahler, 1994; Coats et al., 1996), Thau Lagoon (Sete, France; Chambouvet et al., 2011b), Nauset Marsh system (Massachusetts, USA; Velo-Suarez et al., 2013), Penzé Estuary (Bretagne, France; Chambouvet et al., 2008) and the oligotrophic Mediterranean Sea (Siano et al., 2011). Morphologies of infected hosts are consistent with the aforementioned taxonomic groups in Salt Pond. Nine Group II Syndiniales clades were found to co-occur and included clades 16, 39, and 44, which have no known hosts.

Infections in multiple dinoflagellate morphotypes and the mixed assemblage of Group II Syndiniales parasites obscured specific host-parasite infection dynamics within cohort 1. Sequences annotated to Group II Clade 2 were abundant on 3 July and appeared to infect thecate dinoflagellate morphotypes, like Heterocapsa sp. and Scrippsiella sp., and small (10 µm) athecate cells that could not be identified microscopically. Heterocapsid morphotypes (Fig. S3A-G) represented 17.76% of protists (130 000 cells L1), and of these cells, 4.72% were infected by Group II syndinian parasites. Scrippsielloid morphotypes (Fig. S3H-M) were 9.60% of all protists enumerated (16 000 cells L1), and of these cells, 16.52% were infected (Fig. S4). Multiple host morphologies suggest that clade 2 parasites are either

generalists or the clade is composed of multiple species. collectively capable of infecting multiple protist hosts. Indeed, 51 ASV sequences are annotated to clade 2 parwhich suggests sub-clade variability (Cai et al., 2020). The 13 August infection event involved mixed assemblages of both hosts and parasite clades. Notably, increased parasite diversity (Fig. S4) was correlated with higher infection levels (Fig. 4). This infection event impacted the largest fraction of the in situ protist community (2.56%) and was associated with multiple clades of Group II Syndiniales. Of the dominant morphotypes, 15.75% of the community was heterocapsid cells (160 000 cells L1) and 15.1% of cells with this morphology were infected. Clades 1, 2, 4, 5, 14, 22 and other unassigned Group II sequences were present in iTag libraries and may have contributed to observed infections of hosts with diverse morphologies (Fig. S5). Putative hosts for clades 1, 2, 4, and 14 include Alexandrium sp. Gonyaulax sp., Gymnodinium sp., Heterocapsa sp., and Scrippsiella sp. (Coats et al., 1996; Chambouvet et al., 2008; Siano et al., 2011). Observed infections of small thecate and athecate cells suggest that the host ranges of these parasites may include other taxa that cannot be easily identified morphologically (Fig. S3T-Z). To date, clades 5 and 22 have no identified hosts and our observations of these strains in Salt Pond underscore the technical challenges that remain when characterizing ecological niches for many syndinian parasites.

Syndinian parasite infections impacted the largest fraction of the protist community on 13 August. In addition, the protist community transitioned from dinoflagellatedominated to diatom- and ciliate-dominated. Syndinian parasites can exert top-down pressure on their protist hosts and may stimulate microbial growth through the release of dissolved and particulate organic matter during host cell lysis (Guillou et al., 2008). Other studies of host-parasite systems have shown host-cell lysis contributes to increased nutrient availability and the growth of microbes in the surrounding water column (Salomon et al., 2009; Warren et al., 2010; Berdjeb et al., 2018; Frainer et al., 2018). Parasitism may have influenced the shift toward diatom genera in cohort 2 in mid-August, where lysis of host dinoflagellates contributed to nutrient hotspots, although other driving forces, such as temperature and nutrient shifts driven by intensified stratification, cannot be ruled out. Ammonium, nitrate and nitrite measurements collected during this transition do not indicate large fluxes in nitrogen concentrations. The diatom genera in cohort 2 differed from early spring diatoms (dominated by Thalassiosira, Pinnularia, and Leptocylindrus) and included the cosmopolitan and chain-forming taxa Chaetoceros, Navicula, and Skeletonema. Growth, chain-formation (in the case of Skeletonema and

Chaetoceros) and photosynthetic activity of these diatoms are influenced by factors that include nutrient availability (e.g. nitrate, phosphate, silicate; Karthikeyan et al., 2013; Liu et al., 2013; Zhao et al., 2014; Wang et al., 2020). The diatoms observed in cohort 2 did not appear to be parasitized by Group II Syndiniales targeted by the ALV01 probes.

Ciliate taxa were also abundant and diverse in cohort 2, although no parasitism by Group II Syndiniales was observed in samples from our study. These included Frontonia, Aspidisca, and Strombidium, Parasitic relationships between ciliates and Group II Syndiniales have been hypothesized for coastal ciliate populations based on co-occurrence patterns (Torres-Beltran et al., 2018). It is possible that ciliate species targeted by Group II Syndiniales were not present in Salt Pond, or similarly, that ciliates may have been infected by Syndiniales Group II clades that are not targeted by the CARD-FISH probe we used. Another possibility is that ciliates and Group II Syndiniales may co-occur in other datasets because of grazing and not parasitic interactions (Anderson and Harvey, 2020). Microscopy data before and after 13 August suggest that free-living Syndiniales parasite spores were rapidly removed (Fig. 4). Although we do not have direct evidence for increased grazing on parasite spores by the ciliates in cohort 2, grazing may explain their rapid removal following this infection event.

Cohort 3 spanned from late April to late May and represented a period of time with very low infection prevalence based on microscopy, as well as relatively fewer Syndiniales sequences in marker gene libraries. The composition of cohort 3 included many species of chlorophytes and stramenopiles (Table S3). Of course, parasitism by other parasitic groups may also occur throughout the year. Chytrid fungi, known to infect diatoms (Peacock et al., 2014; Frenken et al., 2017; Kilias et al., 2020), were among cohort 3. The community shifts from diatom-chytrid to dinoflagellate-Syndiniales co-occurrences documented in Salt Pond may represent population succession mediated by seasonal environmental triggers and/or the effects of top-down control of Syndiniales and fungal parasitism on host populations.

The community shift toward cohort 4 occurred around 14 September and was composed of recurring protist taxa including ciliates, chlorophytes, diatoms, MAST stramenopiles, and dinoflagellates that were present in both early spring and early fall. Cohort 4 was distinct from communities during the July and August infection events. Microscopic observations confirmed infected hosts included larger athecate dinoflagellates (25 µm size; Fig. S3N–S) compared to smaller athecate hosts and thecate hosts observed during July and August. The large athecate cell morphotype represented 25.21% of the protist community during the peak of the infection

event, although cells were not heavily infected (2.43% on 14 September; Fig. S4). Cells with this morphology increased to 73.52% of the protist community by 20 September, suggesting that the parasitic infections observed on 14 September did not exert significant topdown pressure on this specific protist population. Cohort 4 included Group II Syndiniales clades (26, 30, 32) that differed from the other cohorts, suggesting host selectivity and/or specific ecological niches. Abiotic factors, including cooler temperatures, shorter day lengths, increased vertical mixing, and nutrient availability are known to influence the periodicity of protists (Lawrence and Menden-Deuer, 2012; Simon et al., 2015) and may explain the appearance of cohort 4 communities both in spring and fall in Salt Pond, and distinct host/parasite assemblages.

#### Conclusion

Syndinian parasites are some of the most abundant and poorly characterized protists across the global ocean, representing an ecological 'black-box' in models of marine food webs and biogeochemical cycling. Molecular and microscopy observations from this highresolution time series study of water samples from Salt Pond reveal both subtle and more prominent shifts in diversity of Group II Syndiniales as well as putative host populations in a coastal marine setting between March and October 2018. Infections were observed predominantly in small (10-25 µm cell size) thecate and athecate dinoflagellate hosts throughout most of the time series, with larger infection events occurring in July, August, and September. Host morphologies and analyses of co-occurring protist taxa suggested unique host-parasite interactions during each infection event across the time series. Infection events coincided most often with dinoflagellate-dominated protist communities that emerged as stratification intensified in Salt Pond; however, large blooms of individual dinoflagellate populations were not observed in this system. Salt Pond represents a different perspective on the activity of Syndiniales parasites, where infections occurred in host communities that were generally lower in abundance than the intensively studied one-species bloom scenario, but still able to propagate efficiently in complex protist communities. This pattern of host/parasite interaction may be more representative of many other marine environments where blooms of single taxa are not the general observation. This theory, and hypotheses regarding generalist versus specific host/parasite associations, will benefit from expanding microscopy studies to other sites and applying single-cell genomic approaches.

# Methods

#### Study site

Salt Pond (Falmouth, MA; 41.5430N, 70.6269W; Supplementary Fig. S1) is within 2 miles of Woods Hole Oceanographic Institution and easily accessible by small row boat, thus facilitating the sampling frequency needed for a high-resolution time series that can capture most parasite infection dynamics. This estuarine system is approximately 5.5 m deep at the sampling site for this study, tidally influenced by the Vineyard Sound, and receives freshwater inputs primarily from groundwater. Salt Pond is seasonally stratified, with oxygen-depleted waters that occur within 2-3 m of the water surface in late summer, and bottom waters that become increasingly sulfidic as stratification intensifies in late summer (reaching up to 5 mM; Wakeham et al., 1984, 1987, Zemmelink et al., 2006).

#### Sample collection

Water samples were collected approximately every 3 days between March and October 2018, which captured periods of increased primary productivity (spring and fall blooms) and seasonal stratification (summer). The pond was sampled at three depths at every time point. These depths correspond to the depths of oxic (2 m), oxycline (3 m), and anoxic (4 m) water conditions that occur during peak stratification. Temperature, salinity, and dissolved oxygen concentrations were profiled using a handheld YSI (YSI Pro2030, OH, USA). Two replicate 1.7 | GoFlo (General Oceanics, FL, USA) casts were performed at each depth. From each cast, 600 ml of seawater was preserved using a final concentration of 4% unbuffered formalin. The 11 of seawater from each cast was kept on ice and returned to the laboratory within 1 h of collection.

In the laboratory, samples from each 1 I sample were processed and stored for amplicon and nitrogen analyses. For each cast, a 20 ml subsample of seawater was filtered onto a 47 mm 0.2  $\mu m$  Millipore Isopore filter that was placed directly in a DNeasy PowerWater Kit (Qiagen, USA) bead tube for DNA extraction. Bead tubes were stored at 20C until extractions were performed. Seawater was processed for water chemistry analyses by filtering through a 0.2  $\mu m$  Sterivex filter, and collecting 50 ml in a HDPE Nalgene bottle for measuring ammonium, nitrate and nitrite concentrations. These HDPE bottles were stored at 20C until analysed on an O.I. Analytical Flow Solutions IV auto analyser at the Louisiana State University Wetland Biogeochemistry Analytical Services facility. Corresponding formalin-fixed seawater samples were subsampled to visualize both free-living parasites and infected hosts. The 20 ml of

formalin-fixed seawater was filtered onto a 47 mm 0.2  $\mu$ m Millipore Isopore filter (black) for enumeration of free-living parasite spores. Filters were rinsed three times with 5 ml of phosphate buffered saline (PBS, 1) and stored at 20C. To enumerate infected hosts, 100 ml or 200 ml (determined by filtering time) of fixed seawater was filtered onto a 47 mm 3.0  $\mu$ m Millipore Isopore filter, rinsed three times with PBS and stored at 20C.

# Catalysed reporter deposition fluorescence in situ hybridization (CARD-FISH)

Filters for enumerating infected hosts and numbers of dinospores were hybridized to a horseradish peroxidase oligonucleotide probe targeting 73 of the 125 clades of Group II Syndiniales (Cai et al., 2020; ALV01). Filters were cut into eight wedges and one wedge per sample was placed on a glass slide. The 20  $\mu$ l of hybridization containing 40% formamide (Chambouvet et al. 2008) and the probe ALV01 (5°-GCC TGC CGT GAA CAC TCT30; Chambouvet et al. 2008) in a 9:1 ratio (final concentration 50 ng µl<sup>1</sup>) was placed on each filter piece and spread using the side of a pipette tip. Slides were placed into 50 ml Falcon tubes on their side with a Kimwipe placed at the bottom of the chamber satu-rated with 1 ml of hybridization buffer. Samples were incubated for a minimum of 8 h at 37C. Following the ini-tial hybridization, filter pieces were washed in 3 ml of a freshly prepared wash solution twice at 46C to remove unhybridized probe, then soaked in 3 ml of Tris-HCl-NaCl-Tween20 (1 M Tris-HCl pH 7.5, Tween20, 5 M NaCl; TNT) buffer at room temperature and placed on a second glass slide. Filters were transferred to new glass slides and fluorescence was amplified using the Perkin tyramide signal amplification NEL741001KT) according to the manufacturer's instructions, and filters were then washed twice in 3 ml of TNT buffer at 55C to neutralize any residual fluorescein. Filters were placed on a glass slide and Calcofluor White (Sigma Aldrich; final concentration 2.5% [vol/vol]) was used to stain cellulose within the cell wall of thecate dinoflagellates. Filters were stained for 7 min and then washed in 3 ml of water twice for 1 min. Filters were counterstained with the nucleic acid stain propidium iodide and mounted on glass slides with Citifluor mounting media (10 μg ml<sup>1</sup> Citifluor; 20 μl mounting solution per slide). Hybridized filters were stored at 4C. A more detailed description of the protocol can be found at dx. doi.org/10.17504/protocols.io.bsxmnfk6.

# Enumeration of free-living dinospores and infected hosts

All microscope analyses were performed on an Axio Imager M2 epifluorescence microscope (Carl Zeiss,

Germany). Hybridized filters were viewed using the FITC filter set, which excites the fluorescein stain coupled to the CARD-FISH probe targeting both free-living parasites and infected cells. The DAPI filter set was used to visualize the presence or absence of host thecae stained with Calcofluor White, and the Cv3 filter set was used to detect the propidium iodide stain and confirm the presence of a nucleus in all putative parasite cells. Free-living parasite spores, hybridized with the ALV01 probe, were enumerated under 400 magnification by counting all spores on 1/8-filter wedges. To calculate overall protist community infection levels within the fraction of the eukaryotic community 10 µm or larger), cells on filters were also hybridized with the ALV01 probe. All infected protist cells showing one or more infective spores within the cell were counted at 400 magnification. All eukary-otic cells within the ocular grid observed at 1000 were counted until either 400 protists or 40 grids were reached. A 'cells per grid' value was calculated and multiplied by the total number of grids on 1/8 of the filter, which was calibrated by comparing the ocular grid to a stage micrometre slide, to estimate total protist abundance. Values for numbers of infected hosts are expressed as the average percent of the total protist community infected based on counts performed for the two replicate casts at each depth. The ALV01 probe sequence was aligned with all Group II Syndiniales marker gene library sequences to qualitatively identify potential underestimates of parasite prevalence.

# DNA extraction and iTag sequencing

DNA was extracted with the Qiagen DNeasy PowerWater kit following the manufacturer's protocols, eluted in a final volume of 50 µl, quantified using a Qubit Fluorometer, and stored at 20C. The 339 samples with sufficient DNA extracted were selected for sequencing and shipped Georgia Genomics and Bioinformatics (University of Georgia) for iTag barcoding and sequencing on the Illumina MiSeq platform using primers for the V4 hypervariable region of the eukaryotic 18S rRNA gene, V4F (50-CCA GCA SCY GCG GTA ATT CC-30; Stoeck et al., 2010) and V4RB (50-ACT TTC GTT CTT GAT YRR-3°; Balzano et al. 2015). The QIIME2 platform and the dada2 pipeline were used to process the sequence data (Bolyen et al., 2019). Reads were quality checked and chimeras were removed. Amplicon sequence variants (ASVs) were clustered based on 100% similarity and representative sequences were aligned and annotated using the PR2 (Guillou et al., 2008) database following standard procedures (Bolyen et al., 2019). All sequences were submitted to GenBank and made publicly available (BioProject ID PRJNA736596).

#### Statistical analyses

All statistical analyses were performed in RStudio (Version 1.1.456) using R (Version 3.6.1). ITag barcode libraries were manually curated, removing amplicon sequence variants (ASVs) that could not be identified to phylum and those annotated to Metazoa and macroalgae. Libraries from replicate casts collected at the same depth on each sampling date were combined.

To evaluate changes in community composition across the time series, non-metric multidimensional scaling was performed using the MASS package (v7.3-51.6; Venables and Ripley, 2002) in R. ASV read counts were transformed using the Hellinger method using decostand in the vegan package (v2.4-2; Oksanen et al., 2017). A dissimilarity index was then constructed using the Bray-Curtis method using vegdist. Points were fitted using isoMDS in the MASS package, which is based on the Kruskal method. Environmental parameters, including temperature, salinity, dissolved oxygen, ammonium, nitrate and nitrite, moon phase, day length, average wind speed, maximum gust, and wind direction were fitted to the points on the ordination plot using the envfit function in the vegan package with 999 permutations. Abiotic factors with P-values less than 0.05 are presented. A correlation matrix of environmental parameters constructed using the rcorr function in the Hmisc package (v4.6-0; Harrell, 2021) in R. Significantly correlated parameters (P < 0.05) are summarized in Fig. S2.

The ASV read count table was then used to determine clusters of co-occurring protist taxa and the temporal dynamics of these community clusters using methods outlined by Coenen et al. (2019). Read counts were normalized to scale and detrend the data. Variances were stabilized so that they no longer correlated with ASV abundances using the varianceStabilizingTransformation function in the DeSeq2 package (v1.39.0; Love et al., 2014). Linear trends were removed using the detrend function in the pracama package (v2.3.3; Borchers, H.W.) and count values were rescaled. The normalized data, or Z-scores, were used to generate a Euclidean distance matrix with the dist function in the stats package (v3.6.2; R Core Team), and to subsequently define protistan community clusters. Clusters were defined using the k-medoids method with the pam function in the cluster package (v2.1.2; Maechler et al., 2021). All scripts used for this analysis can be found at https://github.com/ trsehein/SaltPond iTagAnalysis.

#### Acknowledgements

The authors would like to thank David Beaudoin, Emily Maness, Sarah Lott, Emma Keeler, Rebecca Cox, and Carmine Riccardi for their assistance collecting and processing samples. Thank you to Dr. Jeff Donnelly and Ed Lott for donating

boats for sample collection and the occasional rescue. Thank you to Dr. Sarah Hu for her guidance analysing marker gene libraries and for determining patterns of cooccurring taxa. The authors thank Dr. Paraskevi Mara for her helpful comments on the manuscript and assistance in the field. This material is based upon work supported by the National Science Foundation Biological Oceanography OCE-1851012 to R.G., M.P. and V.E. and by the National Science Foundation Graduate Research Fellowship under Grant No. 1745302.

#### References

- Anderson, S.R., and Harvey, E.L. (2020) Temporal variability and ecological interactions of parasitic marine Syndiniales in coastal protist communities. Msphere 5(3): e00209-20.
- Arístegui, J., Gasol, J.M., Duarte, C.M., and Herndl, G.J. (2009) Microbial oceanography of the dark ocean's pelagic realm. Limnol Oceanogr 54: 1501-1529.
- Bachvaroff, T.R., Kim, S., Guillou, L., Delwiche, C.F., and Coats, D.W. (2012) Molecular diversity of the syndinean genus Euduboscquella based on single-cell PCR analysis. Appl Environ Microbiol 78: 334-345.
- Balzano, S., Abs, E., and Leterme, S.C. (2015) Protist diversity along a salinity gradient in a coastal lagoon. Aquat Microb Ecol 74: 263-277.
- Bazylinski, D.A., Schlezinger, D.R., Howes, B.H., Frankel, R. B., and Epstein, S.S. (2000) Occurrence and distribution of diverse populations of magnetic protists in a chemically stratified coastal salt pond. Chem Geol 169: 319-328.
- Berdjeb, L., Parada, A., Needham, D.M., and Fuhrman, J.A. (2018) Short-term dynamics and interactions of marine protist communities during the spring-summer transition. ISME J 12: 1907-1917.
- Bolyen, E., Rideout, J.R., Dillon, M.R., Bokulich, N.A., Abnet, C.C., Al-Ghalith, G.A., et al. (2019) Reproducible, interactive, scalable and extensible microbiome data science using QIIME 2. Nat Biotechnol 37: 852-857.
- Bråte, J., Krabberød, A.K., Dolven, J.K., Ose, R.F., Kristensen, T., Bjørklund, K.R., and Shalchian-Tabrizi, K. (2012) Radiolaria associated with large diversity of marine alveolates. Protist 163: 767-777.
- Cachon, J. (1964) Contribution à l'étude des péridiniens parasites. Cytologie, cycles évolutifs. Ann Sci Nat Zool 6:1-158.
- Cachon, J., and Cachon, M. (1970) Ultrastructure des Amoebophryidae (Péridiniens Duboscquodinida) Systèmes atractophriens et microtubulaires; leur intervention dans la mitose. Protist 6: 57-70.
- Cai, R., Kayal, E., Alves-De-Souza, C., Bigeard, E., Corre, E., Jeanthon, C., et al. (2020) Cryptic species in the parasitic Amoebophrya species complex revealed by a polyphasic approach. Sci Rep 10: 1-11.
- Carstensen, J., Klais, R., and Cloern, J.E. (2015) Phytoplankton blooms in estuarine and coastal waters: seasonal patterns and key species. Estuar Coast Shelf Sci 162: 98-109.
- Chambouvet, A., Alves-de-Souza, C., Cueff, V., Marie, D., Karpov, S., and Guillou, L. (2011a) Interplay between the parasite Amoebophrya sp.(Alveolata) and the cyst

- formation of the red tide dinoflagellate Scrippsiella trochoidea. Protist 162: 637–649.
- Chambouvet, A., Laabir, M., Sengco, M., Vaquer, A., and Guillou, L. (2011b) B genetic diversity of Amoebophryidae (Syndiniales) during Alexandrium catenella/tamarense (Dinophyceae) blooms in the Thau lagoon (Mediterranean Sea, France). Res Microbiol 162: 959–968.
- Chambouvet, A., Morin, P., Marie, D., and Guillou, L. (2008) Control of toxic marine dinoflagellate blooms by serial parasitic killers. Science 322: 1254–1257.
- Christaki, U., Genitsaris, S., Monchy, S., Li, L.L., Rachik, S., Breton, E., and Sime-Ngando, T. (2017) Parasitic eukaryotes in a meso-eutrophic coastal system with marked Phaeocystis globosa blooms. Front Mar Sci 4: 416.
- Cleary, A.C., and Durbin, E.G. (2016) Unexpected prevalence of parasite 18S rDNA sequences in winter among Antarctic marine protists. J Plankton Res 38: 401–417.
- Coats, D.W., Adam, E.J., Gallegos, C.L., and Hedrick, S. (1996) Parasitism of photosynthetic dinoflagellates in a shallow subestuary of Chesapeake Bay, USA. Aquat Microb Ecol 11: 1–9.
- Coats, D.W., and Bockstahler, K.R. (1994) Amoebophrya ceratii in Chesapeake Bay populations of Gymnodinium sanguineum. J Euk Microbiol 41: 586–593.
- Coats, D.W., and Park, M.G. (2002) Parasitism of photosynthetic dinoflagellates by three strains of Amoebophrya (Dinophyta): parasite survival, infectivity, generation time, and host specificity. J Phycol 38: 520–528.
- Coenen, A.R., Hu, S.K., Luo, E., Muratore, D. & Weitz, J.W. (2019) A Primer for Microbiome Time-Series Analysis. URL https://github.com/shu251/analyzing\_microbiome\_ timeseries
- De Vargas, C., Audic, S., Henry, N., Decelle, J., Mahé, F., Logares, R., et al. (2015) Eukaryotic plankton diversity in the sunlit ocean. Science 348(6237): 1261605.
- Duret, M.T., Pachiadaki, M.G., Stewart, F.J., Sarode, N., Christaki, U., Monchy, S., et al. (2015) Size-fractionated diversity of eukaryotic microbial communities in the eastern tropical North Pacific oxygen minimum zone. FEMS Microbiol Ecol 91. https://doi.org/10.1093/femsec/fiv037
- Edgcomb, V.P. (2016) Marine protist associations and environmental impacts across trophic levels in the twilight zone and below. Curr Opin Microbiol 31: 169–175.
- Edgcomb, V.P., Orsi, W., Bunge, J., Jeon, S.-O., Christen, R., Leslin, C., et al. (2011) Protistan microbial observatory in the Cariaco Basin, Caribbean. I. Pyrosequencing vs. sanger insights into species richness. ISME J 5: 1344–1356.
- Frainer, A., McKie, B.G., Amundsen, p.A., Knudsen, R., and Lafferty, K.D. (2018) Parasitism and the biodiversity-functioning relationship. Trends Ecol Evol 33: 260–268.
- Frenken, T., Alacid, E., Berger, S.A., Bourne, E.C., Gerphagnon, M., Grossart, H.P., et al. (2017) Integrating chytrid fungal parasites into plankton ecology: research gaps and needs. Environ Microbiol 19: 3802–3822.
- Galluzzi, L., Bertozzini, E., Penna, A., Perini, F., Garcés, E., and Magnani, M. (2010) Analysis of rRNA gene content in the Mediterranean dinoflagellate Alexandrium catenella and Alexandrium taylori: implications for the quantitative real-time PCR-based monitoring methods. J Appl Phycol 22: 1–9.

- Gong, W., and Marchetti, A. (2019) Estimation of 18S gene copy number in marine eukaryotic plankton using a next-generation sequencing approach. Front Mar Sci 6: 219.
- Guillou, L., Viprey, M., Chambouvet, A., Welsh, R., Kirkham, A.R., Massana, R., et al. (2008) Widespread occurrence and genetic diversity of marine parasitoids belonging to Syndiniales (Alveolata). Environ Microbiol 10: 3349–3365.
- Harrell, F.E. (2021) Hmisc: Harrell Miscellaneous. R package version 4.6-0 URL https://CRAN.R-project.org/package= Hmisc
- Jacobson, D.M. (1987) The Ecology and feeding biology of thecate heterotrophic dinoflagellates. Doctoral dissertation: Woods Hole, MA, USA: Woods Hole Oceanographic Institution.
- Jephcott, T.G., Alves-de-Souza, C., Gleason, F.H., van Ogtrop, F.F., Sime-Ngando, T., Karpov, S.A., and Guillou, L. (2016) Ecological impacts of parasitic chytrids, syndiniales and perkinsids on populations of marine photosynthetic dinoflagellates. Fungal Ecol 19: 47–58.
- Jin, J., Liu, S.M., Ren, J.L., Liu, C.G., Zhang, J., and Zhang, G.L. (2013) Nutrient dynamics and coupling with phytoplankton species composition during the spring blooms in the Yellow Sea. Deep Sea Res 2 Top Stud Oceanogr 97: 16–32.
- Karthikeyan, P., Manimaran, K., Sampathkumar, P., and Rameshkumar, L. (2013) Growth and nutrient removal properties of the diatoms, Chaetoceros curvisetus and C. simplex under different nitrogen sources. Appl Water Sci 3: 49–55.
- Kilias, E.S., Junges, L., Šupraha, L., Leonard, G., Metfies, K., and Richards, T.A. (2020) Chytrid fungi distribution and co-occurrence with diatoms correlate with sea ice melt in the Arctic Ocean. Commun Biol 3: 1–13.
- Kim, S. (2006) Patterns in host range for two strains of Amoebophrya (Dinophyta) infecting thecate dinoflagellates: Amoebophrya spp. ex Alexandrium affine and ex Gonyaulax polygramma. J Phycol 42: 1170–1173.
- Kim, S., Park, M.G., Kim, K.Y., Kim, C.H., Yih, W., Park, J. S., and Coats, D.W. (2008) Genetic diversity of parasitic dinoflagellates in the genus Amoebophrya and its relationship to parasite biology and biogeography. J Euk Microbiol 55: 1–8.
- Kremp, A., Tamminen, T., and Spilling, K. (2008) Dinoflagellate bloom formation in natural assemblages with diatoms: nutrient competition and growth strategies in Baltic spring phytoplankton. Aquat Microb Ecol 50: 181–196.
- Lawrence, C., and Menden-Deuer, S. (2012) Drivers of protistan grazing pressure: seasonal signals of plankton community composition and environmental conditions. Mar Ecol Prog Ser 459: 39–52.
- Li, C., Song, S., Liu, Y., and Chen, T. (2014) Occurrence of Amoebophrya spp. infection in planktonic dinoflagellates in Changjiang (Yangtze River) estuary. China Harmful Algae 37: 117–124.
- Lin, S. (2011) Genomic understanding of dinoflagellates. Res Microbiol 162: 551–569.
- Liu, Y., Song, X., Cao, X., and Yu, Z. (2013) Responses of photosynthetic characters of Skeletonema costatum to different nutrient conditions. J Plankton Res 35: 165–176.

- Lopez-García, P., Rodríguez-Valera, F., Pedros-Alio, C., and Moreira, D. (2001) Unexpected diversity of small eukaryotes in deep-sea Antarctic plankton. Nature 409: 603-607.
- Love, M.I., Huber, W., and Anders, S. (2014) Moderated estimation of fold change and dispersion for RNA-seq data with DESeq2. Genome Biol 15(550): 10-1186.
- Maechler, M., Rousseeuw, P., Struyf, A., Hubert, M., and Hornik, K. (2021) Cluster: cluster analysis basics and extensions. R package version 22.
- Mallin, M.A., Paerl, H.W., and Rudek, J. (1991) Seasonal phytoplankton composition, productivity and biomass in the Neuse River estuary North Carolina. Estuar Coast Shelf Sci 32: 609-623.
- Maranda, L. (2001) Infection of Prorocentrum minimum (Dinophyceae) by the parasite Amoebophrya sp.(Dinoflagellata). J Phycol 37: 245-248.
- Margalef, R., Estrada, M., and Blasco, D. (1979) Functional morphology of organisms involved in red tides, as adapted to decaying turbulence. In Toxic Dinoflagellate Blooms, Taylor, D., and Seliger, H. (eds). New York, NY: Elsevier, pp. 89-94.
- Massana, R., Balagué, V., Guillou, L., and Pedros-Alio, C. (2004) Picoeukaryotic diversity in an oligotrophic coastal site studied by molecular and culturing approaches. FEMS Microbiol Ecol 50: 231-243.
- Miller, J.J., Delwiche, C.F., and Coats, D.W. (2012) Ultrastructure of Amoebophrya sp. and its changes during the course of infection. Protist 163: 720-745.
- Moskowitz, B.M., Bazylinski, D.A., Egli, R., Frankel, R.B., and Edwards, K.J. (2008) Magnetic properties of marine magnetotactic bacteria in a seasonally stratified coastal pond (Salt Pond, MA, USA). Geophys J Int 174: 75-92.
- Nishitani, L., Erickson, G., and Chew, K.K. (1985) Role of the parasitic dinoflagellate Amoebophrya ceratii in control of Gonyaulax catenella populations. Toxic dinoflagellates. New York, USA: Elsevier Science Publishers, pp. 225-230.
- Not, F., del Campo, J., Balagué, V., de Vargas, C., and Massana, R. (2009) New insights into the diversity of marine picoeukaryotes. PloS ONE 4: e7143.
- Not, F., Gausling, R., Azam, F., Heidelberg, J.F., and Worden, A.Z. (2007) Vertical distribution of picoeukaryotic diversity in the Sargasso Sea. Environ Microbiol 9: 1233-1252.
- Oksanen, J., Blanchet, F.G., Kindt, R., Legendre, P., Minchin, p.R., O'hara, R.B., et al. (2017) Vegan: community ecology package. R package
- Orsi, W., Song, Y.C., Hallam, S., and Edgcomb, V.P. (2012) Effect of oxygen minimum zone formation on communities of marine protists. ISME J 6: 1586-1601.
- Pawlowski, J., Audic, S., Adl, S., Bass, D., Belbahri, L., Berney, C., et al. (2012) CBOL protist working group: barcoding eukaryotic richness beyond the animal, plant, and fungal kingdoms. PLoS Biol 10: e1001419.
- Peacock, E.E., Olson, R.J., and Sosik, H.M. (2014) Parasitic infection of the diatom Guinardia delicatula, a recurrent and ecologically important phenomenon on the New England shelf. Mar Ecol Prog Ser 503: 1-10.
- Pernice, M.C., Giner, C.R., Logares, R., Perera-Bel, J., Acinas, S.G., Duarte, C.M., et al. (2015) Large variability of bathypelagic microbial eukaryotic communities across the world's oceans. ISME J 10: 945-958.

- Pernice, M.C., Logares, R., Guillou, L., and Massana, R. (2013) General patterns of diversity in major marine microeukaryote lineages. PLoS ONE 8: e57170.
- Prokopowich, C.D., Gregory, T.R., and Crease, T.J. (2003) The correlation between rDNA copy number and genome size in eukaryotes. Genome 46: 48-50.
- Salomon, p.S., Granéli, E., Neves, M.H., and Rodriguez, E. G. (2009) Infection by Amoebophrya spp. parasitoids of dinoflagellates in a tropical marine coastal area. Aquat Microb Ecol 55: 143-153.
- Sassenhagen, I., Irion, S., Jardillier, L., Moreira, D., and Christaki, U. (2020) Protist interactions and community structure during early autumn in the Kerguelen region (Southern Ocean). Protist 171: 125709.
- Scholz, B., Guillou, L., Marano, A.V., Neuhauser, S., Sullivan, B.K., Karsten, U., et al. (2016) Zoosporic parasites infecting marine diatoms-a black box that needs to be opened. Fungal Ecol 19: 59-76.
- Sengco, M.R., Coats, D.W., Popendorf, K.J., Erdner, D.L., Gribble, K.E. and Anderson, D.M. (2003) Biological and phylogenetic characterization of Amoebophrya sp. ex Alexandrium tamarense. In Second Symposium on Harmful Marine Algae in the US, Abstract (Vol. 57).
- Siano, R., Alves-de-Souza, C., Foulon, E., Bendif, E.M., Simon, N., Guillou, L., and Not, F. (2011) Distribution and diversity of Amoebophryidae parasites across oligotrophic waters of the Mediterranean Sea. Biogeosciences 8: 267-278.
- Silva, A., Palma, S., Oliveira, p.B., and Moita, M.T. (2009) Composition and interannual variability of phytoplankton in a coastal upwelling region (Lisbon Bay, Portugal). J Sea Res 62: 238-249.
- Simmons, S.L., Bazylinski, D.A., and Edwards, K.J. (2007) Population dynamics of marine magnetotactic bacteria in a meromictic salt pond described with qPCR. Environ Microbiol 9: 2162-2174.
- Simmons, S.L., Sievert, S.M., Frankel, R.B., Bazylinski, D. A., and Edwards, K.J. (2004) Spatiotemporal distribution of marine magnetotactic bacteria in a seasonally stratified coastal salt pond. Appl Environ Microbiol 70: 6230-6239.
- Simon, M., Lopez-García, P., Deschamps, P., Moreira, D., Restoux, G., Bertolino, P., and Jardillier, L. (2015) Marked seasonality and high spatial variability of protist communities in shallow freshwater systems. ISME J 9: 1941-1953.
- Skovgaard, A. (2014) Dirty tricks in the plankton: diversity and role of marine parasitic protists. Acta Protozool 53: 51-62.
- Skovgaard, A., Massana, R., Balague, V., and Saiz, E. (2005) Phylogenetic position of the copepod-infesting parasite Syndinium turbo (Dinoflagellata, Syndinea). Protist 156: 413-423.
- Smayda, T.J., and Reynolds, C.S. (2003) Strategies of marine dinoflagellate survival and some rules of assembly. J Sea Res 49: 95-106.
- Spilling, K., Olli, K., Lehtoranta, J., Kremp, A., Tedesco, L., Tamelander, T., et al. (2018) Shifting diatomdinoflagellate dominance during spring bloom in the Baltic Sea and its potential effects on biogeochemical cycling. Front Mar Sci 5: 327.
- Stentiford, G.D., and Shields, J.D. (2005) A review of the parasitic dinoflagellates Hematodinium species and

- Hematodinium-like infections in marine crustaceans. Dis Aquat Organ 66: 47–70.
- Stoeck, T., Bass, D., Nebel, M., Christen, R., Jones, M.D., Breiner, H.W. and Richards, T.A. (2010) Multiple marker parallel tag environmental DNA sequencing reveals a highly complex eukaryotic community in marine anoxic water. Mol Ecol 19: 21–31.
- Stoecker, D.K., Hansen, p.J., Caron, D.A., and Mitra, A. (2017) Mixotrophy in the marine plankton. Ann Rev Mar Sci 9: 311–335.
- Suter, E.A., Pachiadaki, M., Taylor, G.T., and Edgcomb, V.P. (2022) Eukaryotic parasites are integral to a productive microbial food web in oxygen-depleted waters. Front Microbiol 4166: 12:764605. https://doi.org/10.3389/fmicb. 2021.764605
- Sverdrup, H.U. (1953) On conditions for the vernal blooming of phytoplankton. J Cons Int Explor Mer 18: 287–295.
- Torres-Beltran, M., Sehein, T., Pachiadaki, M.G., Hallam, S.J., and Edgcomb, V. (2018) Protistan parasites along oxygen gradients in a seasonally anoxic fjord: a network approach to assessing potential host-parasite interactions. Deep Sea Res 2 Top Stud Oceanogr 156: 97–110.
- Trigueros, J.M., and Orive, E. (2001) Seasonal variations of diatoms and dinoflagellates in a shallow, temperate estuary, with emphasis on neritic assemblages. Hydrobiologia 444: 119–133.
- Velo-Suarez, L., Brosnahan, M.L., Anderson, D.M., and McGillicuddy, D.J., Jr. (2013) A quantitative assessment of the role of the parasite Amoebophrya in the termination of Alexandrium fundyense blooms within a small coastal embayment. PLoS ONE 8: e81150.
- Venables, W.N., and Ripley, B.D. (2002) Modern Applied Statistics with S, 4th ed. New York, NY: Springer ISBN 0-387-95457-0.
- Wakeham, S.G., Howes, B.L., and Dacey, J.W. (1984) Dimethyl sulphide in a stratified coastal salt pond. Nature 310: 770–772.
- Wakeham, S.G., Howes, B.L., Dacey, J.W.H., Schwarzenbach, R.P., and Zeyer, J. (1987) Biogeochemistry of dimethylsulfide in a seasonally stratified coastal salt pond. Geochim Cosmochim Acta 51: 1675–1684.
- Wang, H., Chen, F., Mi, T., Liu, Q., Yu, Z., and Zhen, Y. (2020) Responses of marine diatom Skeletonema marinoi to nutrient deficiency: programmed cell death. Appl Environ Microbiol 86(3): e02460-19.
- Warren, C.P., Pascual, M., Lafferty, K.D., and Kuris, A.M. (2010) The inverse niche model for food webs with parasites. Theor Ecol 3: 285–294.
- Yoshie, N., Yamanaka, Y., Kishi, M.J., and Saito, H. (2003)
  One dimensional ecosystem model simulation of the effects of vertical dilution by the winter mixing on the spring diatom bloom. J Oceanogr 59: 563–571.

- Zemmelink, H.J., Houghton, L., Frew, N.M., and Dacey, J.W. H. (2006) Dimethylsulfide and major sulfur compounds in a stratified coastal salt pond. Limnol Oceanogr 51: 271–270
- Zhao, X., Pang, S., Liu, F., Shan, T., and Li, J. (2014) Biological identification and determination of optimum growth conditions for four species of Navicula. Acta Oceanol Sin 33: 111–118.
- Zhou, Y., Zhang, Y., Li, F., Tan, L., and Wang, J. (2017) Nutrients structure changes impact the competition and succession between diatom and dinoflagellate in the East China Sea. Sci Total Environ 574: 499–508.

# **Supporting Information**

Additional Supporting Information may be found in the online version of this article at the publisher's web-site:

Figure S1 A map displaying the sampling point and the location of Salt Pond (Falmouth, MA; 41.5430N, 70.6269W).

Figure S2 Correlation matrix of the environmental variables measured in Salt Pond. Bubble colour and size are proportional to the correlation coefficients. Bubbles are only presented for correlated variables with significance values p < 0.05.

Figure S3 A selection of infected cells imaged during the three larger infection events. Parasites are labelled with the CARD-FISH probe ALVO1 and stained green when observed with a FITC filter set. Host theca are stained with Calcofluor when present and blue when visualized with a DAPI filter. Both host and parasite nuclei are stained with propidium iodide and are red when viewed with a Cy3 filter set. (a-g) cells with heterocapsid morphology, (h-m) cells with scrippsielloid morphology, (n-s) cells with shared athecate morphology, and (t-z) other interesting, but less common, infection morphotypes. All scale bars denote 5 µm.

#### Figure \$4

Figure S5 The relative abundance of Group II Syndiniales clade reads at two meters during three infection events.

Table S1 A summary of the environmental parameters and water column chemistry measured for each sample cast. Sample identifiers correspond to the date, followed by the cast (C) replicate number and the depth (D; 1 = 2 m, 2 = 3 m, 3 = 4 m).

Table S2 Raw read counts from all ASVs generated by the dada2 pipeline and annotated using the PR2 database. Sample identifiers correspond to the date, followed by the cast (C) replicate number and the depth (D; 1 = 2 m, 2 = 3 m, 3 = 4 m).

Table S3 The taxonomic composition of the co-occurring protist cohorts generated by the k-medoids clustering analysis.